

Infrared studies of the evolution of the CiOi(Sil) defect in irradiated Si upon isothermal anneals

Angeletos, T. , Chroneos, A. and Londos, C. A.

Author post-print (accepted) deposited in CURVE May 2016

Original citation & hyperlink:

Angeletos, T. , Chroneos, A. and Londos, C. A. (2016) Infrared studies of the evolution of the CiOi(Sil) defect in irradiated Si upon isothermal anneals. Journal of Applied Physics, volume 119 : 125704

<http://dx.doi.org/10.1063/1.4945110>

DOI 10.1063/1.4945110

ISSN 0021-8979

ESSN 1089-7550

Publisher: American Institute of Physics

This article may be downloaded for personal use only. Any other use requires prior permission of the author and AIP Publishing.

The following article appeared in Angeletos, T. , Chroneos, A. and Londos, C. A. (2016) Infrared studies of the evolution of the CiOi(Sil) defect in irradiated Si upon isothermal anneals. Journal of Applied Physics, volume 119 : 125704 and may be found at [http://dx.doi.org/ 10.1063/1.4945110](http://dx.doi.org/10.1063/1.4945110)

Copyright © and Moral Rights are retained by the author(s) and/ or other copyright owners. A copy can be downloaded for personal non-commercial research or study, without prior permission or charge. This item cannot be reproduced or quoted extensively from without first obtaining permission in writing from the copyright holder(s). The content must not be changed in any way or sold commercially in any format or medium without the formal permission of the copyright holders.

This document is the author's post-print version, incorporating any revisions agreed during the peer-review process. Some differences between the published version and this version may remain and you are advised to consult the published version if you wish to cite from it.

IR studies of the evolution of the $C_iO_i(Si_I)$ defect in irradiated Si upon isothermal anneals

T. Angeletos¹, A. Chroneos^{2,3,a} and C. A. Londos^{1,b}

¹*University of Athens, Solid State Physics Section, Panepistimiopolis Zografos, Athens 157 84, Greece*

²*Faculty of Engineering, Environment and Computing, Coventry University, Priory Street, Coventry CV1 5FB, United Kingdom*

³*Department of Materials, Imperial College London, London SW7 2AZ, United Kingdom*

Abstract

Carbon-oxygen-self-interstitial complexes were investigated in silicon by means of Fourier Transform infrared (FTIR) spectroscopy. Upon irradiation, the C_iO_i defect (C_3) forms, which for high doses attracts self-interstitials (Si_I 's) leading to the formation of the $C_iO_i(Si_I)$ defect (C_4) with two well-known related bands at 939.6 and 1024 cm^{-1} . The bands are detectable in the spectra both in room temperature (RT) and liquid helium (LH) temperatures. Upon annealing at 150 °C, these bands were transformed to three bands at 725, 952 and 973 cm^{-1} , detectable only at LH temperatures. Upon annealing at 220 °C, these bands were transformed to three bands at 951, 969.5 and 977 cm^{-1} , detectable both at RT and LH temperatures. Annealing at 280 °C, resulted in the transformation of these bands to two new bands at 973 and 1024 cm^{-1} . The latter bands disappear from the spectra upon annealing at 315 °C without the emergence of other bands in the spectra. Considering reaction kinetics and defect metastability we developed a model to describe the experimental results. Annealing at 150 °C triggers the capturing of Si_I 's by the C_4 defect leading to the formation of the $C_iO_i(Si_I)_2$ complex. The latter structure appears to be bistable: measuring at LH the defect is in configuration $C_iO_i(Si_I)_2$ giving rise to the bands at 725, 952 and 973 cm^{-1} , whereas on measurements at RT the defect converts to another configuration $C_iO_i(Si_I)_2^*$ without detectable bands in the spectra. Possible structures of the two $C_iO_i(Si_I)_2$ configurations are considered and discussed. Upon annealing at 220 °C additional Si_I 's are captured by the $C_iO_i(Si_I)_2$ defect leading to the formation of the $C_iO_i(Si_I)_3$ complex, which in turn on annealing at 280 °C converts to the

$C_iO_i(Si_I)_4$ complex. The latter defect anneals out at 315°C, without being accompanied in the spectra by the growth of new bands.

Keywords: silicon; carbon; oxygen; defects; electron irradiation; FTIR

^{a)}Electronic mail: alexander.chroneos@imperial.ac.uk

^{b)}Electronic mail : hlontos@phys.uoa.gr

1. Introduction

There is extensive research and technological interest on oxygen (O) and carbon (C) impurities in Si, which are unintentionally introduced in the lattice during crystal growth.¹ Upon irradiation O and C associate to form the most important carbon-oxygen related defect the C_iO_i defect (C_3).² For high irradiation doses the C_iO_i center acts^{2,3} as a nucleation center for Si_I 's leading to the formation of the $C_iO_i(Si_I)$ complex (C_4) and thereafter to larger complexes such as the $C_iO_i(Si_I)_2$, $C_iO_i(Si_I)_3$, and so on. More generally, numerical modeling of experimental data regarding irradiation of carbon contained Cz-Si on increased doses showed^{3,4} that Si_I 's could be captured successively by the initially formed C_iO_i and C_iC_s pairs leading to the formation of larger $C_iO_i(Si_I)_n$ and $C_iC_s(Si_I)_n$ clusters. The latter large complexes are also expected to form on thermal anneals of the $C_iO_i(Si_I)$ and the $C_iC_s(Si_I)$ defects, which are the first members correspondingly of these families of defects. The $C_iC_s(Si_I)$ complexes are beyond the scope of the present study.

Regarding the $C_iO_i(Si_I)_n$ family and in particularly the evolution of the bands appearing in the IR spectra upon isochronal anneals and the defects related with these bands, there are different opinions in the literature and a complete picture has not been reached so far. In one hand measurements carried out both at cryogenic and RT measurements have shown a complicated annealing behavior^{5,6} of the C_4 defect, as it

appears in the infrared (IR) spectra. Indeed, it was reported^{5, 6} that in low temperature measurements, carried out in the course of 30 min isochronal anneals, the two bands at 940 and 1024 cm^{-1} related with the C_4 defect formed upon irradiation are transformed when the annealing temperature reaches ~ 200 °C to a second group of three bands at 724, 952 and 973 cm^{-1} , which in turn at ~ 250 - 275 °C are transformed to a another third group of three bands at 951, 969 and 977 cm^{-1} . The latter bands disappear from the spectra at ~ 300 - 325 °C without the appearance of new bands in the spectra. In RT measurements⁵ the first group of two bands appears at 936 and 1020 cm^{-1} . Importantly the second group of bands is not observable in the spectra. It has been suggested^{5,6} that the above three groups of bands are related to three different configurations C_4 , C_4^* and C_4^{**} of the initial $C_iO_i(\text{Si}_i)$ (C_4) structure, which upon increasing the annealing temperature is thermally transformed to more stable configurations ($C_4 \rightarrow C_4^* \rightarrow C_4^{**}$). On the other hand, density functional theory (DFT) calculations^{7,8} questioned the above conclusion. Indeed, all the geometry optimizations converged to three configurations⁸ of the $C_iO_i(\text{Si}_i)$ structure but the calculated localized vibrational modes (LVMs) frequencies are not consistent with the observed⁵ experimental frequencies. Notably, in recent hybrid functional DFT calculations⁹ consistent conclusions to previous theoretical work^{7,8} regarding the $C_iO_i(\text{Si}_i)$ structure were reached.

The picture regarding the $C_iO_i(\text{Si}_i)$ structure is incomplete and additional information is necessary to resolve the above issues. In the present study we have performed isothermal anneals at characteristic temperatures in the range from RT to 315 °C and carried out mainly LH measurements to study the transformations of the $C_iO_i(\text{Si}_i)$ complex. Notably, during anneals at a certain temperature, various reactions among defects can take place controlled by their respective kinetics. These reactions

can lead to metastable states of the defects. Here, we introduce a model regarding the transformations of the $C_iO_i(Si_I)$ complex considering the formation of $C_iO_i(Si_I)_n$, $1 \leq n \leq 4$ complexes, with $C_iO_i(Si_I)_2$ exhibiting a bistable behavior. In particular we suggest that the latter defect switches between two configurations depending on the temperature of the measurement.

2. Experimental method

The samples used in this experiment were cut from prepolished Czochralski-grown Si (Cz-Si) wafers of 2mm thickness with initial oxygen and carbon concentrations $[O_i]_o$ and $[C_s]_o$ of about $6.3 \times 10^{17} \text{ cm}^{-3}$ and $1.3 \times 10^{17} \text{ cm}^{-3}$, respectively. They were calculated from the intensities of the 1107 and 605 cm^{-1} bands of the O_i and the C_s impurities using calibration coefficients^{10, 11} of 3.14×10^{17} and 10^{17} cm^{-2} respectively. They were irradiated with 2 MeV electrons at 80 °C, with a fluence of $5 \times 10^{17} \text{ cm}^{-2}$ using the Dynamitron accelerator at Takasari-JAERI (Japan). After the irradiation the samples were placed in a quartz tube to avoid contamination and then inserted in an open furnace where they were subjected to isothermal anneals at 150, 220, 280 and 315 °C. At each one of these temperatures, several anneals of one or two hours duration were carried out. After each annealing step, the IR spectra were taken at LH temperatures (~ 10 K) by using a JASCO-470 plus FTIR spectrometer operated with a resolution of 1 cm^{-1} . The evolution of the present bands was monitored carefully. The two-phonon intrinsic absorption was always subtracted in each spectrum making use of a float-zone sample of equal thickness. The IR spectra reported below refers to the same sample subjected successively to thermal treatments, that is isothermal anneals at the various temperatures mentioned above.

3. Results and discussion

Fig. 1 presents the IR spectrum of a representative sample before and after irradiation taken at LH temperature. IR bands of the VO (835 cm^{-1}), the C_iO_i (865 cm^{-1}) and the C_4 ($939.6, 1024\text{ cm}^{-1}$) bands are shown.

Fig. 2 presents a series of IR spectra taken at LH temperature after isothermal anneals at $150\text{ }^\circ\text{C}$. It shows the gradual disappearance of the 939.6 and 1024 cm^{-1} bands of the C_4 and the emergence in the course of anneals of a second group of bands at $725, 952$ and 973 cm^{-1} . Suggestions on the structure of the latter defect will be discussed below. Importantly, these bands do not appear in RT measurements.^{5, 6} In relation with that we note that earlier studies of RT measurements in neutron irradiated Si, have reported¹² two bands of the C_4 defect at 934 and 1018 cm^{-1} . These bands begin to disappear from the spectra upon isochronal anneals at temperatures above $150\text{ }^\circ\text{C}$ without the emergence of accompanied bands in the spectra, in agreement with the results reported by Murin *et al.*^{5, 6} Additionally, two bands at 945 and 964 cm^{-1} were detected¹² to arise in the spectra $\sim 230\text{ }^\circ\text{C}$. The latter two bands, corresponding with two bands of the third group reported^{5, 6} above, have been tentatively correlated¹³ with the $\text{C}_i\text{C}_s(\text{Si}_i)_2$ structure,

Fig. 3 presents a series of IR spectra taken at LH temperature after isothermal anneals at $220\text{ }^\circ\text{C}$. It shows the gradual disappearance of the bands at $725, 952$ and 973 cm^{-1} and the emergence in the course of anneals of a third group of bands at $951, 969.5$ and 977 cm^{-1} . Suggestions on the structure of the latter defect will be discussed in what follows.

Fig. 4 presents a series of IR spectra taken after isothermal anneals at $280\text{ }^\circ\text{C}$. It shows the gradual disappearance of the bands at $951, 969.5$ and 977 cm^{-1} and the emergence in the course of anneals of a fourth group of bands at 973 and 1024 cm^{-1} .

Again suggestions on the structure of the defect that gives origin of the latter bands will be discussed below.

Fig. 5 presents a series of IR spectra taken after isothermal anneals at 315 °C. It shows the gradual disappearance of the bands at 973 and 1024 cm⁻¹. After 10h anneals at 315 °C, these two bands disappear from the spectra without being accompanied by the growth of new bands. Notably, the latter group of bands was not reported by Murin *et al.*^{5,6} either in LH or in RT measurements. Nevertheless, a band at 1020 cm⁻¹ has been reported¹⁴ to appear in the spectra of RT measurements in a sequence of 20min isochronal anneals treatments. The band emerges above ~250 °C and disappears from the spectra above ~ 450 °C.

To gain a clearer perspective of the phenomenon we introduce Fig. 6, which presents the evolution of all the IR bands observed in the spectra in the course of the series of isothermal anneals at 150, 220, 280 and 315 °C. The values in the lower x-axis represent the total anneal time irrespective of the temperature of anneal and should be read with care. For instance, the value of t=12h corresponds to the sample subjected to thermal treatments at 150 °C for 9h and subsequently at 220 °C for 3h. Similarly, the value 20h means that the same sample was subjected to isothermal anneals at 150 °C for 9h, at 220 °C for 7h and at 280 °C for 4h.

The above observations have led us to suggest the following model. On thermal treatment at 150 °C as the annealing time increases LH measurements show that the two bands of the first group of bands (939.6 and 1024 cm⁻¹) are gradually replaced in the spectra by the three bands of the second group (725, 952 and 973 cm⁻¹). In the course of annealing various reactions may take place. Since C₄ is a relatively large complex it is not likely⁵ to diffuse as a unit in the Si lattice. Additionally, there are no indications⁵ of any dissociation of the defect and therefore it is reasonable to

consider that other defects present could move and react with the C_4 defect. A strong candidate may be Si_I 's being released^{15, 16} from di-interstitial pairs. They could be captured by C_4 to form the complex $C_iO_i(Si_I)_2$, via the reaction $C_iO_i(Si_I) + Si_I \rightarrow C_iO_i(Si_I)_2$.

At this point it is necessary to consider the picture of the spectra in relation with the temperature of the measurement. The fact that the bands (725, 952 and 973 cm^{-1}) of the second group do not appear^{5,6} in the RT measurements, is a strong indication that the $C_iO_i(Si_I)_2$ defect exhibits characteristics of bistability^{17,18} transforming between two different configurations. Such changes are characteristic of second order phase transitions.¹⁹ Notably, here we observe that in our case due to the irradiation, the Fermi level is pinned⁵ in the middle of the forbidden gap and therefore the conversion from one configuration to the other cannot occur due to changes in the charge state of the defect, since it is permanently in one charge state. Interestingly, it has been reported²⁰ in the literature a kind of metastability, where the defect switches from one configuration to another due to changes in the temperature of the sample, as a result of entropy variations along the path of the configuration change. In general, for a defect to transform from one configuration to another it has to surpass an energy barrier. In other words, at a certain temperature, the two configurations of the defect are separated by an energy barrier and the stable configuration of the defect is that where the Gibbs free energy G (where $G = H - ST$, H and S are the formation enthalpy and entropy) of its formation has an absolute minimum. In case that the entropy of the defect varies with temperature, then at a certain critical temperature $\Delta H = T\Delta S$ occurs, where no barrier separates anymore the two configurations. Above that temperature the other configuration prevails²⁰ to which the defect is now converted.

Measurements of the spectra at LH and RT verify the existence of the three bands in the first case and the lack of any bands in the second.

Fig. 7 presents a characteristic IR spectrum received with RT measurements after annealing at 150 °C, for 8h. Notice that the values of the two bands of the $C_iO_i(Si_i)$ defect are now at RT at 1020 and 936 cm^{-1} . Comparing Fig. 7 with Fig. 2 which was received with LH measurements after the same thermal treatment, we observe that the second group of bands at 725, 952 and 973 cm^{-1} is not present in Fig. 7. In a first attempt to interpret the results, it can be suggested that entropy driven variations govern the behavior of the $(C_iO_i(Si_i)_2)$ defect, as it appears from the picture in the IR spectra received at LH and RT measurements. The latter structure appears to convert from one configuration $C_iO_i(Si_i)_2$ (725, 952 and 973 cm^{-1}) with LH measurements to another configuration $C_iO_i(Si_i)_2^*$ (without detectable LVMs) with RT measurements. In this model, one expects that the conversion occurs at a characteristic critical T where $\Delta H = T\Delta S$. Of course, systematic studies are required to determine the exact value of this temperature. Suggestions for the possible geometries of the two $C_iO_i(Si_i)_2$ structures will be discussed below.

On thermal treatments at 220 °C (see Fig.3) as the annealing time increases LH measurements show that the three bands of the second group (725, 952 and 973 cm^{-1}) gradually replaced in the spectra by the three bands of the third group (951, 969.5 and 977 cm^{-1}). In the same train of thought as described above, and considering previous models^{3,4,21,22} where simulation of experimental data suggested the sequential capturing of Si_i 's by the $C_iO_i(Si_i)$ defect, we consider that additional Si_i 's are captured by the $C_iO_i(Si_i)_2$ leading to the formation of a $C_iO_i(Si_i)_3$ complex according to the reaction $C_iO_i(Si_i)_2 + Si_i \rightarrow C_iO_i(Si_i)_3$. Furthermore, on thermal treatments at 280 °C (see Fig. 4), the three bands of the third group (951, 969.5 and 977 cm^{-1}) give place

to a fourth group of bands at 973 and 1024 cm^{-1} originated from the $\text{C}_i\text{O}_i(\text{Si}_i)_4$, which forms when Si_i 's are captured by the $\text{C}_i\text{O}_i(\text{Si}_i)_3$ according to the reaction $\text{C}_i\text{O}_i(\text{Si}_i)_3 + \text{Si}_i \rightarrow \text{C}_i\text{O}_i(\text{Si}_i)_4$. Sources of these Si_i 's can be large defect clusters, formed in the course of irradiation, that contain Si_i 's in their structure.²³ Recent studies²⁴ have suggested the tetra-interstitial cluster as a potential candidate.

On thermal treatments at 315 °C the latter two bands disappear from the spectra without the emergence of new bands (see Fig. 5). One possibility is that the signals from a $\text{C}_i\text{O}_i(\text{Si}_i)_5$ structure formed from the reaction $\text{C}_i\text{O}_i(\text{Si}_i)_4 + \text{Si}_i \rightarrow \text{C}_i\text{O}_i(\text{Si}_i)_5$ are very weak and pass undetectable. It is also likely that the $\text{C}_i\text{O}_i(\text{Si}_i)_n$ complex cannot accommodate more than 4 Si_i 's. Thus, the $\text{C}_i\text{O}_i(\text{Si}_i)_4$ structure collapses possibly dissociating to its constituents C, O and Si_i 's. The release of Si_i 's is expected to cause changes in the concentration of C_iO_i and VO defects due to the reactions $(\text{C}_s + \text{Si}_i \rightarrow \text{C}_i, \text{C}_i + \text{O}_i \rightarrow \text{C}_i\text{O}_i)$ in the former case and the reaction $(\text{VO} + \text{Si}_i \rightarrow \text{O}_i)$ in latter case. Fig. 8 presents the evolution of the C_iO_i and VO defects upon isochronal annealing at 315 °C. Nevertheless, any indications from these curves to support the above argumentation cannot be deduced. This point requires further investigation.

Fig. 9 is a schematic representation of the successive $\text{C}_i\text{O}_i(\text{Si}_i)_n$ $1 \leq n \leq 4$ structures as they transform from one member of the family to the next in the course of annealing at certain temperatures, of the present experiment. It represents the variation of the Gibbs free energy G versus a reaction coordinate throughout the reaction path that the defect is converting from the initial $\text{C}_i\text{O}_i(\text{Si}_i)$ complex to the final $\text{C}_i\text{O}_i(\text{Si}_i)_4$ complex. The suggested bistability of the $\text{C}_i\text{O}_i(\text{Si}_i)_2$ structure is depicted by an insert configurational coordinate diagram representing the transformation of the latter defect between LH and RT measurements.

In support of the above suggestion, it is important to study and discuss the structure of the successive members of the $C_iO_i(Si_I)_n$ family of defects. In order to do that, it is necessary to begin with the structure of the C_iO_i defect. This appears in two forms²⁵ where in the first one the O_i is divalent (O-form) (Fig. 10(a)) and in the second the O_i is trivalent (R-form) (Fig. 10(b)). The label R comes from the geometrical configuration of the defect where the O_i , C_i and two Si lattice atoms form a ring. The $C_iO_i(Si_I)$ structure results from the attachment of a Si_I atom in the C_iO_i defect. At least three configurations of this defect have been discussed^{8, 26, 27} in the literature, which are represented on Fig. 10(c),(d),(e). The Si_I is attached at the side of the C_i atom^{7, 8}. Carbon is far more electronegative than Si, so Si_I prefers to bond with the C_i atom than with the Si(2) atom. In addition, C has a smaller covalent radius than that of the Si so there is more space available for the Si_I atom to be placed next to the carbon atom. The $C_iO_i(Si_I)$ structure is similar to the C_iO_iH defect²⁷ where the Si_I atom replaces the H atom. In the first $C_iO_i(Si_I)$ configuration Fig. 10(c) the Si(2) atom and the O_i atom are separated, although in the second configuration with the Si(2) atom and the O_i -atom are bonded, Fig. 10(d). These two configurations of the $C_iO_i(Si_I)$ are produced^{26,27} from the two configurations (O-form and R-form) correspondingly of the C_iO_i pair (Fig.10 (a),(b)). The third configuration of the $C_iO_i(Si_I)$ depicted in Fig. 10(e), is an alternative structure suggested by Estreicher and Backlund^{7,8} where O and C atoms are bonded in an R-form again.

Upon annealing at 150 °C an additional Si_I atom is captured by the $C_iO_i(Si_I)$ defect to form a $C_iO_i(Si_I)_2$ structure, which can be thought of as being similar to the $C_iO_iH_2$.²⁷ Among several alternative structures the energetically favorable structure has the arrangement where the second Si_I atom binds with the Si(2) on the opposite side of the O_i atom (refer to Fig. 10(f)). In this configuration the Si(2)– Si_I bond is

perpendicular to the C–Si_I bond. A second configuration is that with the Si_I atom in the same side with the O_i atom²⁷ (refer to Fig. 10(g)). Both these structures of the C_iO_i(Si_I)₂ are produced from the O-form of the C_iO_i(Si_I) structure. As mentioned the bistability for the C_iO_i(Si_I)₂ defect, is manifested in the spectra with LVM bands in one configuration attained at LH measurements although there no observed bands in the other configuration attained at RT measurements. The suggested bistability of the C_iO_i(Si_I)₂ is related with the above two configurations of the defect as depicted in Fig. 10(f),(g). Nevertheless, the lack of bands in the second configuration of the C_iO_i(Si_I)₂ defect is not easily reconciled with the above suggestion. Indeed both the configurations of the C_iO_i(Si_I)₂ defect are expected to give rise to IR bands in the spectra. Notably, theoretical studies by Backlund and Estreicher⁸ have shown that some of the IR bands of the C_iO_i(Si_I) defect could be very small.

In the above explanation it was considered that the energy barrier separating the two configurations is temperature-dependent and there exists a critical temperature for which this barrier is eliminated and where the one configuration is fully converted to the other. This, however, is not consistent with the non-detection of the second configuration attained at RT. Thus an alternative explanation may be suggested. Consider again the above two configurations depicted in Fig. 10(f),(g) of the C_iO_i(Si_I)₂ defect. At LH measurements the C_iO_i(Si_I)₂ defect is in the configuration depicted in Fig. 10(f). As the temperature increases the defect transforms to the second configuration depicted in Fig. 10(g). Analogously, to the suggestion of Coutinho *et al.*²⁷ for the C_iO_iH₂ structure were the second configuration of the defect has a higher energy of 0.6 eV we consider that between the two C_iO_i(Si_I)₂ configurations the one represented in Fig. 10(g) is energetically higher than that depicted in Fig. 10(f). In this new model we consider that the barrier that separates the

two configurations does not change substantially with temperature. The probability of transition is analogous to the Boltzmann factor $\exp(-\Delta G/kT)$. Since $\Delta G = \Delta H - T\Delta S$, we have $\exp(-\Delta G/kT) = \exp(-\Delta H/kT) \cdot \exp(\Delta S/k)$. Considering that $\Delta S/k$ is small enough so that it can be neglected, then the energy difference between two configurations is ΔH and the probability of the transition is in essence proportional to $\exp(-\Delta H/kT)$. Thus, considering ΔH to be almost temperature-independent one may suppose that as the temperature increases from LH temperature to RT the $C_iO_i(Si_I)_2$ defects in the first configuration gradually transform to the second. The percentage of the population of the defect occupied by the two configurations changes with the increase of the temperature. The higher the T the lower the ratio between the populations of the two configurations $C_iO_i(Si_I)_2$ and $C_iO_i(Si_I)_2^*$. This means that the population in the second configuration increases with T. In this way of thinking both configurations are expected to be statistically occupied at RT measurements, if the conversion process has not been completed at RT. This in essence results to even lower intensities of the corresponding bands in the spectra and therefore given the weakness of the signals they cannot be detected. The corresponding configuration coordinate diagram is that in Fig. 11 were at RT both configurations of the defect are occupied. On returning now at LH temperatures most of the defect is in the low energy configuration (Fig. 10(f)) and its signals can be detected again in the spectra.

No configurations of the $C_iO_i(H)_2$ defect have been suggested²⁷ as produced correspondingly from the R-form of the $C_iO_i(H)$ structure. Considering, however, that Si_I and H are different species there is the possibility that there is a $C_iO_i(Si_I)_2$ defect being derived from the R-form of the $C_iO_i(Si_I)$ structure. This would just result from the attachment of a Si_I on the R-form of the $C_iO_i(Si_I)$ structure (Fig. 10(d) or (e)). The relatively small energy difference calculated by recent DFT studies^{8,9} between the O-

and R-form of the $C_iO_i(Si_I)$ allows us to consider that the corresponding forms of the $C_iO_i(Si_I)_2$ defect may also be energetically comparable. This suggests that $C_iO_i(Si_I)_2$ defect may switch between the O- and the R-form instead of the two O forms considered above. These aspects motivate further experimental and theoretical studies to verify in one hand the bistability of the $C_iO_i(Si_I)_2$ defect and in the other hand the exact configurations that the defect transforms between LH and RT measurements.

Notably, there is a similarity between the $C_iO_i(Si_I)_n$ and the VO_n ^{28,29} families of defects in Si. Both families are produced after irradiation and subsequent annealing where in the first case in the initial formed $C_iO_i(Si_I)$ complex Si_I 's are attached successively, although in the second case in the initial formed VO pair oxygen atoms are successively added upon anneals. The second member of the VO_n family, the VO_2 defect, exhibits³⁰ bistability where temperature plays a role in the exposed behaviour. Here we suggest that the second member of the $C_iO_i(Si_I)_n$ family, that is the $C_iO_i(Si_I)_2$ complex, exhibits also some kind of bistability, where temperature is the main parameter controlling its behaviour.

Regarding the $C_iO_i(Si_I)_3$ and the $C_iO_i(Si_I)_4$ complexes there are no reports in the literature about their possible structures, in particular the position of the third Si_I in the former defect and the position of the third and fourth Si_I in the latter defect. Second neighbor positions for the additional Si_I are considered as possible arrangements for these structures.

The picture of the $C_iO_i(Si_I)$ defect is incomplete and there are many points to consider.^{7,8} Firstly, the number of the detected LVM bands of the defect is smaller than expected. $C_iO_i(Si_I)$ formed immediately after irradiation has two bands in comparison with the seven bands^{8,26} of the C_iO_i , from which the $C_iO_i(Si_I)$ is produced. Secondly, the C_iO_i is electrical active giving a donor level in the gap, in contrast with

the $C_iO_i(Si_I)$. No electrical activity has been reported experimentally for the $C_iO_i(Si_I)$, although theoretical studies⁸ have predicted a donor level for this defect. Thirdly, the defect exhibits configurational metastability upon annealing but the suggested model^{5,6} from experimental results does not agree with the results from theoretical calculations.^{7,8} The present study attempts to comprehend the metastability of the defect and consider the mechanisms controlling the exhibited behavior. In future work high fluence irradiations of Cz-Si material contained high carbon concentrations are required to study in more detail the weak signals of the $C_iO_i(Si_I)_n$ $1 \leq n \leq 4$ family.

4. Conclusions

In the present study we employ IR spectroscopy to present a systematic study of the evolution of the $C_iO_i(Si_I)$ complex upon isothermal anneals of irradiated Cz-Si contained carbon. Monitoring the successive decay and growth of bands in the course of isothermal anneals we conclude that the evolution of the $C_iO_i(Si_I)$ defect seems to be controlled by reaction kinetics with the successive addition of Si_I creating the $C_iO_i(Si_I)_n$ $1 \leq n \leq 4$ family. Interestingly, the $C_iO_i(Si_I)_2$ structure, exhibits bistability with the defect switching among two configurations on measurements at LH and RT temperatures, respectively. In general, the evolution of the $C_iO_i(Si_I)$ defect and its depicted behavior on thermal treatments has generated a lot of interest not only in the fundamental solid state physics regarding the properties of defects but also on technological issues regarding applications requiring Si devices with certain characteristics.

Acknowledgments

T. Angeletos is grateful to the A.S. Onassis Foundation for financial support through his PhD scholarship (grant No. G ZL 001-1/2015-2016).

References

- ¹V. V. Voronkov, R. Falster, C. A. Londos, E. N. Sgourou, A. Andrianakis, and H. Ohyama, *J. Appl. Phys.* **110**, 093510 (2011); C. A. Londos, E. N. Sgourou, A. Chroneos, and V. V. Emtsev, *Semicond. Sci. Technol.* **26**, 105024 (2011); L. I. Murin, V. P. Markevich, J. L. Lindström, M. Kleverman, J. Hermansson, T. Hallberg and B. G. Svensson, *Solid State Phenom.* **82-84**, 57 (2002); E. N. Sgourou, D. Timerkaeva, C. A. Londos, D. Aliprantis, A. Chroneos, D. Caliste, and P. Pochet, *J. Appl. Phys.* **113**, 113506 (2013); A. Chroneos and C. A. Londos, *J. Appl. Phys.* **107**, 093518 (2010).
- ²G. Davies and R. C. Newman in: T. S. Moss (Ed.), *Handbook in Semiconductors*, Vol.3b Edited by S. Mahajan, Elsevier Science B. V. , Amsterdam, 1994, 1557-1635; C.A. Londos, *Semicond. Sci. Technol.* **5**, 645 (1990); M. R. Brozel, R. C. Newman and D. H. J. Totterdell, *J. Phys. C* **8**, 243 (1975)
- ³G. Davies E. C. Lightowers, R. C. Newman and A. S. Oates, *Semicond. Sci. Technol.* **2**, 524 (1987)
- ⁴A. S. Oates, R. C. Newman, J. M. Tucker, G. Davies and E. C. Lightowers, *MRS* **59**, 59 (1986)
- ⁵L. I. Murin, J. L. Lindstrom, G. Davies, V. P. Markevich, *Nucl. Instrum. Meth. Phys. Res. B* **253**, 210 (2006)
- ⁶L. I. Murin, B. G. Svensson, V. P. Markevich, A. R. Peaker, *Solid State Phenomena* **205-206**, 218 (2014)
- ⁷D. J. Backlund and S. K. Estreicher, *Physica B* **401-402**, 163 (2007)
- ⁸D. J. Backlund and S. K. Estreicher, *Phys. Rev. B* **77**, 205205 (2008)
- ⁹H. Wang, A. Chroneos, C. A. Londos, E. N. Sgourou, and U. Schwingenschlögl, *Sci. Rep.* **4**, 4909 (2014).

- ¹⁰J. L. Regolini, J. P. Stroquert, C. Ganter, and P. Siffert, *J. Electrochem. Soc.* **133**, 2165 (1986)
- ¹¹A. Baghdadi, W. M. Bullis, M. C. Choarkin, Y. Li, R. I. Scace, R. W. Series, P. Stallhofer, and M. Watanabe, *J. Electrochem. Soc.* **136**, 2015 (1989)
- ¹²C. A. Londos, M. S. Potsidi, G. D. Antonaras, A. Andrianakis, *Physica B* **376-377**, 165 (2006)
- ¹³M. S. Potsidi C. A. Londos, *J. Appl. Phys.* **100**, 033523 (2006)
- ¹⁴C. A. Londos, E. N. Sgourou, A. Andrianakis, A. Misiuk, V. V. Emtsev, H. Ohyama, *Solid State Phenomena* **178-179**, 147 (2011)
- ¹⁵Y. H. Lee, *Appl. Phys. Lett.* **73**, 1119 (1998)
- ¹⁶C. A. Londos, G. Antonaras, M. S. Potsidi, D. N. Aliprantis, A. Misiuk, *J. Mater. Sci.: Mater. Electron* **18**, 721 (2007)
- ¹⁷A. Chante, *Appl. Phys. A.* **48**, 3 (1989)
- ¹⁸J. L. Benton, *J. Electron. Mater.* **18**, 199 (1989)
- ¹⁹V. A. Ivanyukovich, V. I. Karas', and V. M. Lomako, *Sov. Phys. Semicond.* **23**, 164 (1989)
- ²⁰B. Hamilton, A. R. Peaker and S. T. Pantelides, *Phys. Rev. Lett.* **61**, 1627 (1988)
- ²¹G. Davies, *Mater. Sci. Forum* **38-41**, 151 (1989)
- ²²S. P. Chappell and R. C. Newman, *Semicond. Sci. Technol.* **2**, 691 (1987)
- ²³R. C. Newman and R. Jones, in *Semiconductors and Semimetals*, edited by F. Shimura (Academic, San Diego, 1994), **42** p. 289
- ²⁴V. Quemener, B. Raeissi, F. Herklotz, L. I. Murin, E. V. Monakhov, and B. G. Svensson, *J. Appl. Phys.* **118**, 135703 (2015)
- ²⁵R. Jones and S. Öberg, *Phys. Rev. Lett.* **68**, 86 (1992)
- ²⁶G. Davies, S. Hayama and S. Hao, B. B. Nielsen, J. Coutinho, M. Sanati, S. K. Estreicher, K. M. Itoh, *Phys. Rev. B* **71**, 115212 (2005)

²⁷J. Coutinho and R. Jones, P. R. Briddon, S. Öberg, L. I. Murin, V. P. Markevich, J. L. Lindström, Phys. Rev. B **65**, 014109 (2002)

²⁸L. I. Murin, J. L. Lindstrom, B. G. Svensson, V. P. Markevich, A. R. Peaker and C. A. Londos, Solid State Phenomena **108-109**, 267 (2005)

²⁹C. A. Londos, L. G. Fytros, G. J. Georgiou, Defect and Diffusion Forum **171-172**, 1 (1999).

³⁰J. L. Lindström, L. I. Murin, B. G. Svensson, V. P. Markevich, T. Hallberg, Physica B **340-342**, 509 (2003).

Figure captions

Fig. 1 Fragments of the IR spectrum of a representative Cz-Si sample before and after measured at LH temperatures.

Fig. 2 Fragments of a series of IR spectra taken at LH temperature after isothermal anneals at 150 °C for certain time durations.

Fig. 3 Fragments of a series of IR spectra taken at LH temperature after isothermal anneals at 220 °C, for certain time durations.

Fig. 4 Fragments of a series of IR spectra taken at LH temperature after isothermal anneals at 280 °C, for certain time durations.

Fig. 5 Fragments of a series of IR spectra taken at LH temperature after isothermal anneals at 315 °C, for certain time durations.

Fig. 6 The evolution of all the IR bands observed in the spectra in the course of the series of isothermal anneals performed at 150, 220, 280 and 315 °C.

Fig. 7 Fragments of the IR spectrum of a representative Cz-Si sample taken at RT temperatures after isothermal anneals at 150 °C for time duration of 8h.

Fig. 8 The evolution of the C_iO_i and VO defects upon isothermal anneal at 315 °C.

Fig. 9 Schematic representation of the $C_iO_i(Si_I)_n$ defect transformations: The variation of the Gibbs free energy throughout the reaction path of the $C_iO_i(Si_I)_n$ defects involving metastability of the $C_iO_i(Si_I)_2$ structure. After the 315 °C anneal no IR bands are observed.

Fig. 10 Various configurations of the C_iO_i (a,b), $C_iO_i(Si_I)$ (c,d,e) and $C_iO_i(Si_I)_2$ (f,g) defects. Black spheres represent C_i and red spheres O_i atoms.

Fig. 11 The configuration coordinate diagram for the case that the two configurations of the $C_iO_i(Si_I)_2$ structure are occupied at RT.

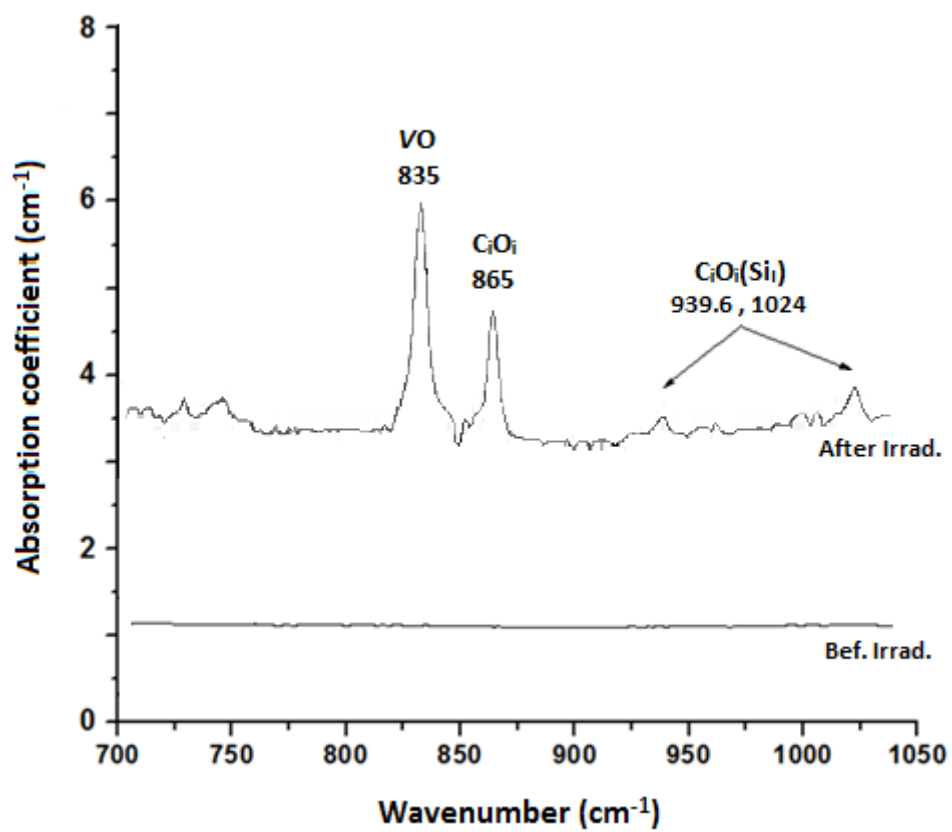


Fig. 1

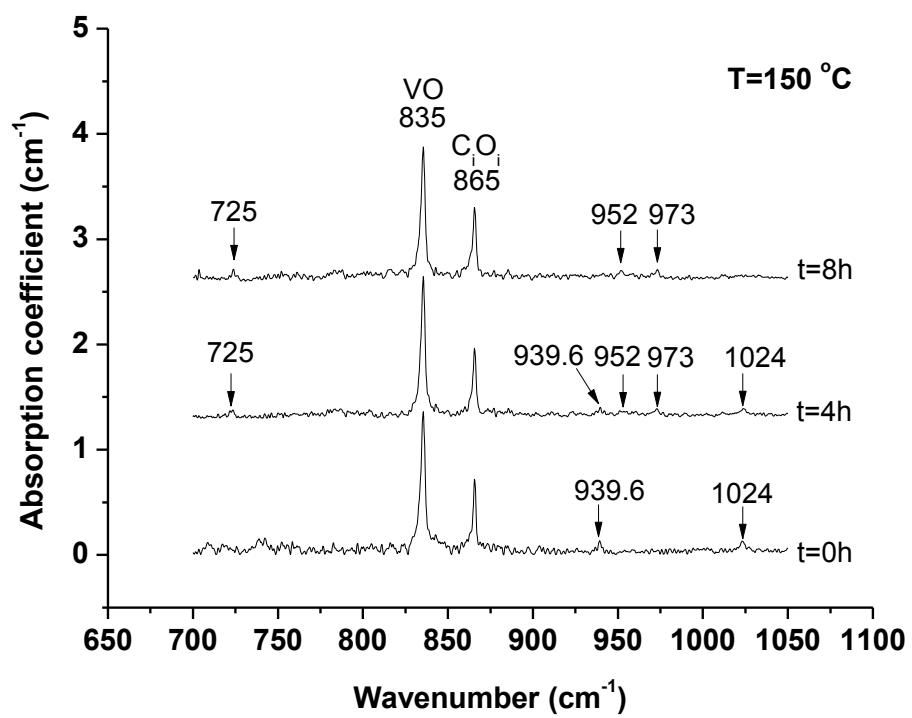


Fig.2

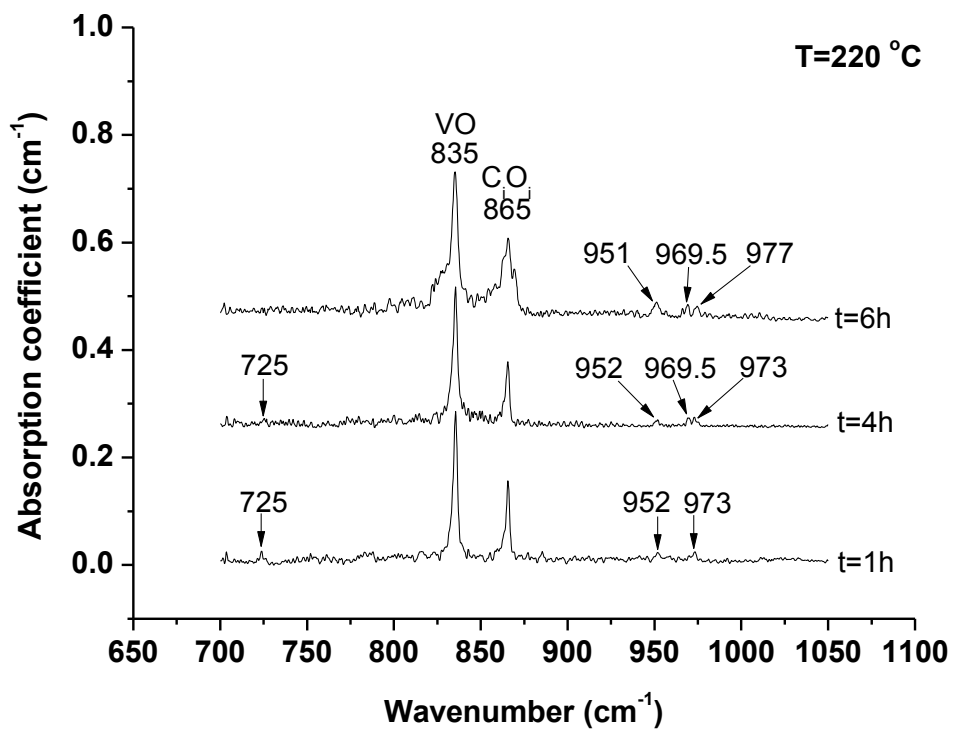


Fig.3

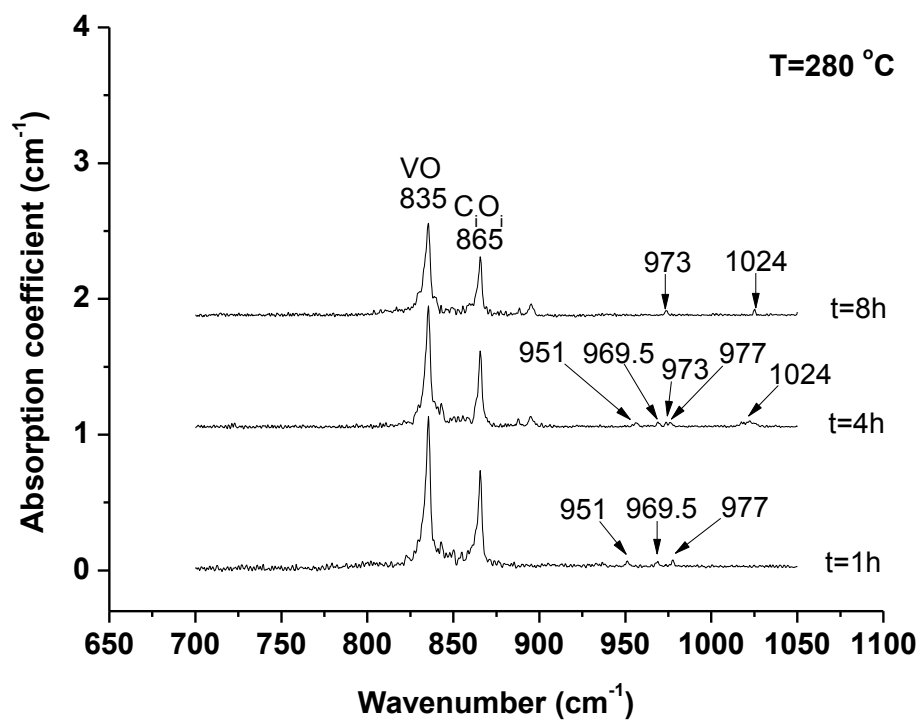


Fig.4

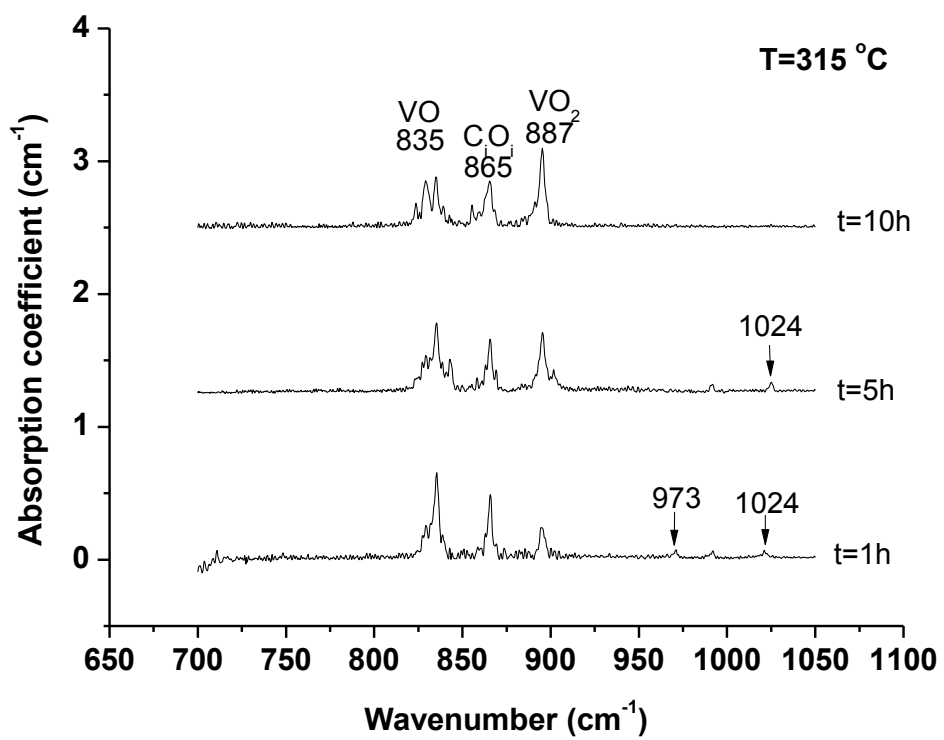


Fig.5

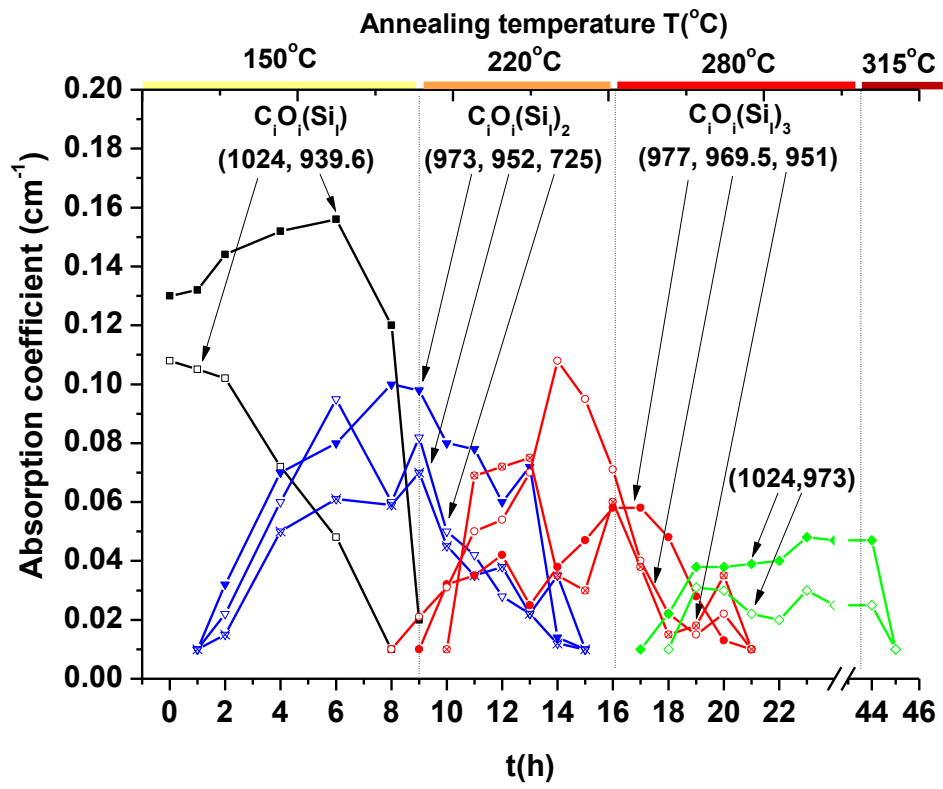


Fig. 6

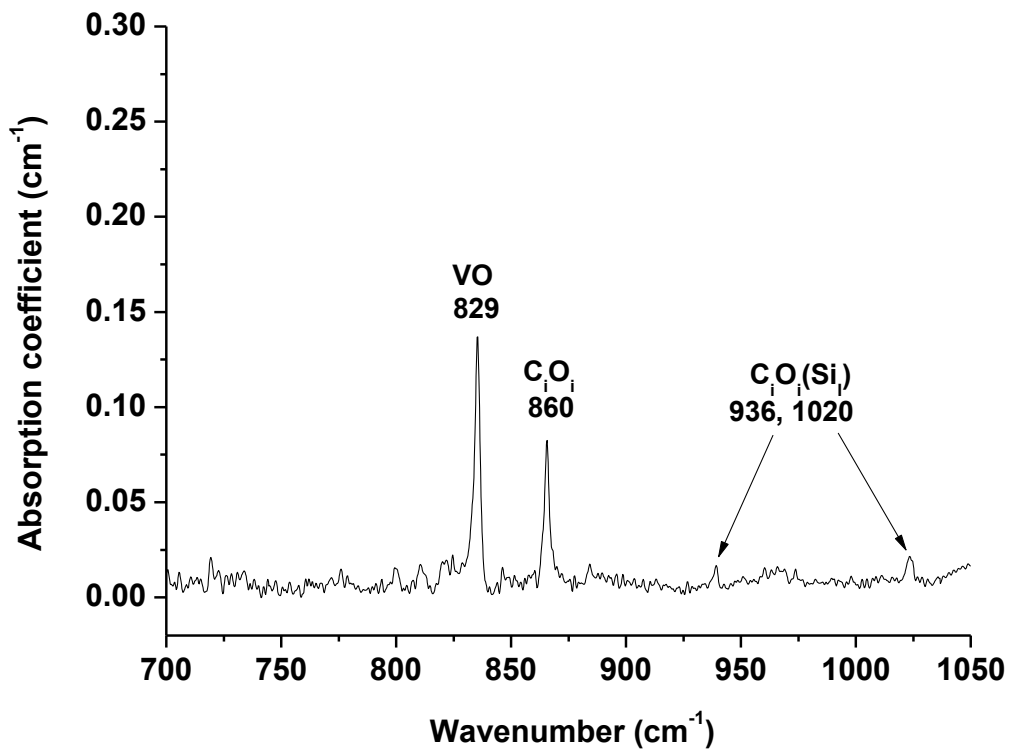


Fig. 7

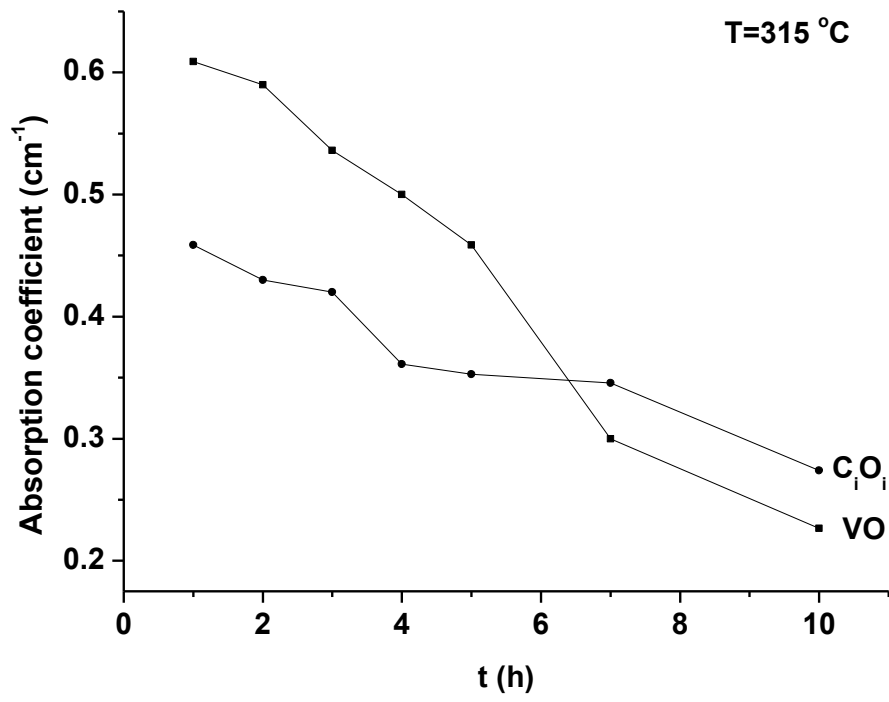


Fig. 8

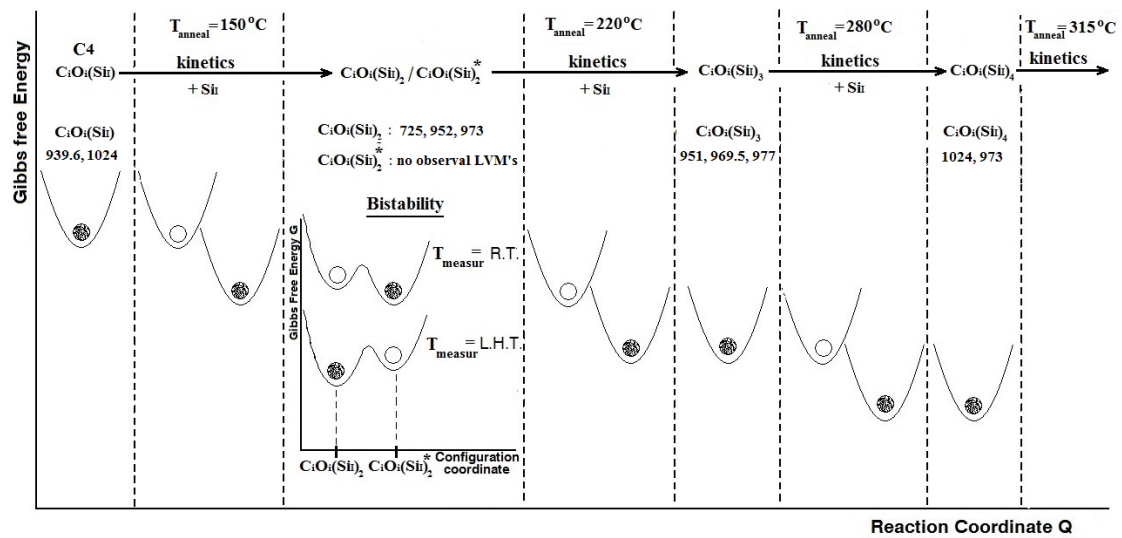


Fig. 9

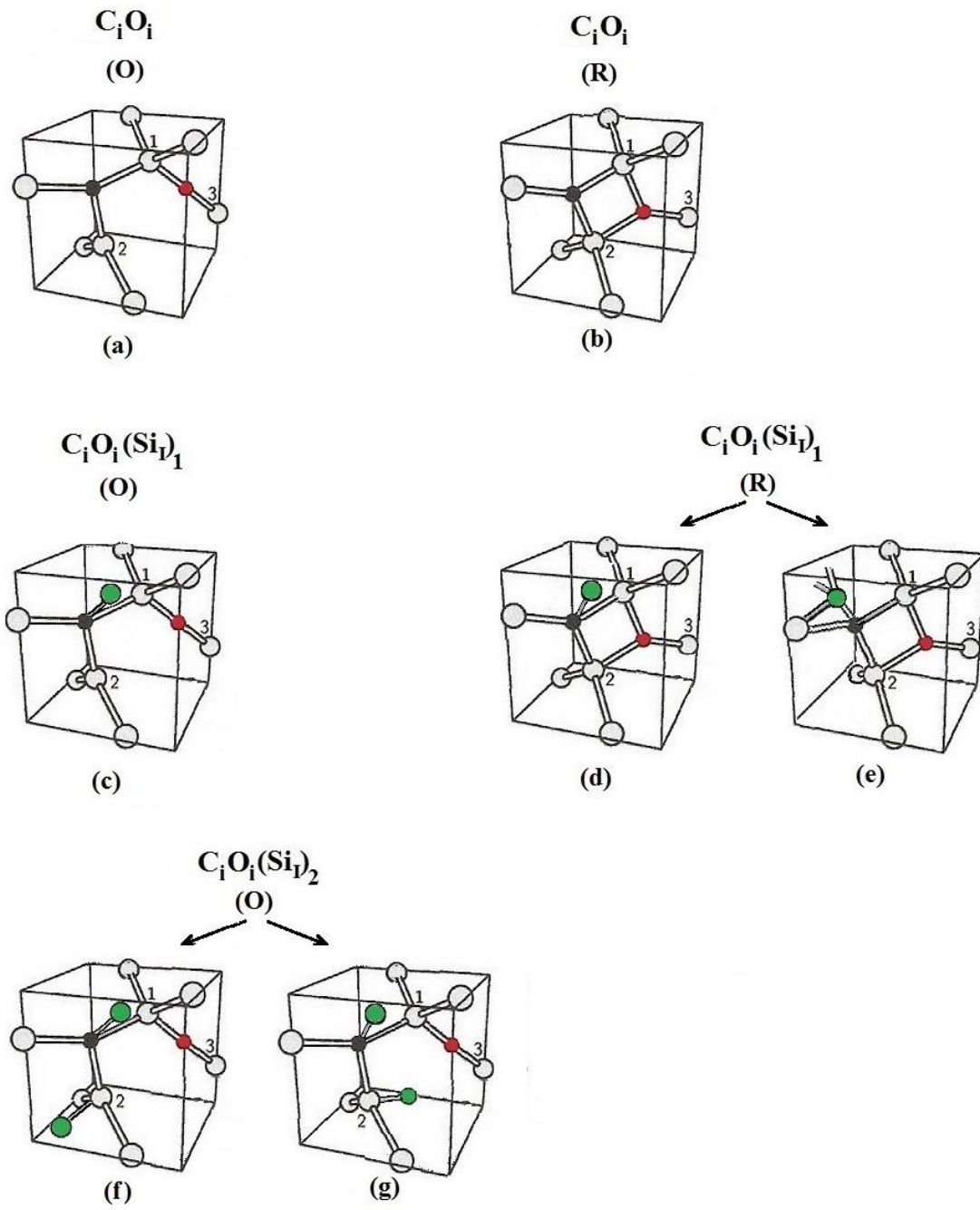


Fig. 10

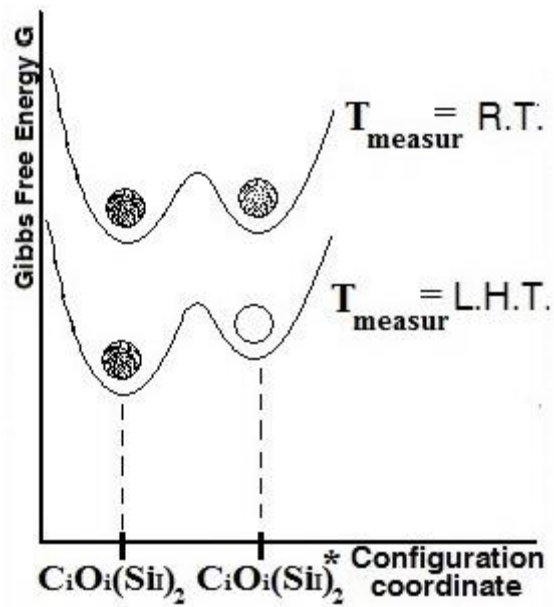


Fig.11